Vibroacoustic loads on spacecraft antennae: analysis and test correlations

J. Santiago-Prowald[1], G. Rodrigues[1] & J.L. Riobóo-Estripot[2]
[1] *Structures Section, ESA-ESTEC, The Netherlands.*
[2] *EADS CASA Espacio, Spain.*

Abstract

The acoustic load during launch is one of the dimensioning cases of spacecraft structures, especially demanding for large antenna reflectors. Current specifications rely on the diffuse field idealisation, while tests are actually performed in reverberating chambers, leading to discrepancies between predicted and measured responses. Most of these are due to the limited capabilities of analytical tools for industrial applications and the testing facilities, particularly when dealing with the modelling or control of the acoustic inputs. However, as shown in this paper, some sources of correlation errors are inappropriate signal processing methods, that do not take into account the physical nature of the loads and the fluid-structure coupling. In particular, digital filtering techniques applied to fine resolution power spectral densities are proposed, in order to better retain the effect of cavity modes, instead of the octave-fraction bands approach. This is of interest when analysing the low frequency range, in which the most important contributions to structural stresses usually appear, depending on the size in terms of pressure blocking, the structural impedance, the acceptance of eigen-mode shapes and the radiation coupling. Several industrial examples are studied, providing insight into typical results, the nature of the discrepancies and some possible solutions.

1 Introduction

Acoustic testing activity in the context of space industry is mostly focused on the integrity of spacecraft and their components when submitted to the acoustic environment of a launch [1]. This load case is particularly relevant for lightweight structural elements, antennae, solar panels and sun shields. The origin of the noise is the sound emission of the propulsion system, the turbulent

jets and the reflections of sound on ground and launch pad at lift-off. Aeroacoustic noise generated during transonic atmospheric flight is also of high intensity, although usually less demanding than lift-off. The acoustic load propagates through the air, as well as the launcher structure, towards the fairing, where payloads are located.

The actual noise during launch is transient in nature and contains pure tones and an intense random background [2]. The airborne propagation is affected by multiple reflections and the presence of the fairing [3]. Despite the complexity of the field inside the fairing, it is usually assimilated to a diffuse field with stationary and ergodic random character. These properties do not respond to reality, although uncertainty is covered by safety factors. The resulting test specifications are typically constant levels within each octave band, applied one to two minutes [4]. The overall SPL is around 146 dB for qualification.

Tests are usually performed in reverberating chambers. The fact that reverberating fields differ from diffuse fields especially at low frequency [5,6,7] is another source of uncertainty, customarily overlooked in common practice.

In this paper a review of the current industrial procedures concerning analytical prediction, testing and their correlation is performed. The purpose is to improve the correlation of test output with prediction, without modifying the current philosophy. Possible sources of error have been identified, related to the acoustic load modelling of the reverberating chamber test. The non-diffusivity at low frequencies couples in a conspicuous manner with structural modes, which are the most important for stress analysis [8]. Furthermore, signal treatment deserves special attention as related to resolution, data reduction and normalisation. Therefore, a digital filter is proposed, providing clear improvements in the correlation task. Analysis and test data have been obtained during the ESA project LARDAL, carried out by EADS-CASA Espacio.

2 The acoustic environment during launch

In the case of Ariane 5, several acoustic sources have been identified [2]:

- At ignition, blast waves propagate along and across the launcher structure inducing lateral vibrations, mainly between 5 and 10 Hz. These overpressures are transient, although treated as a quasi-static load for structural dimensioning.
- At lift-off, the Vulcain main engine and EAP boosters vibrations, as well as the turbulent jet noise and reflections on ground and launch pad, are the sources of excitation. The Vulcain produces an intense 100 Hz tone, while boosters pressure oscillations, attributed to internal cavity modes (1st around 20 Hz, 2nd around 40 Hz), vary in intensity during the combustion time.
- During transonic flight, boundary layer noise is generated. Buffeting in the vehicle aft excites the nozzle pendulum mode at 10 Hz.

Maximum noise levels appear at ignition and lift-off. The pseudo-harmonic vibrations, and their corresponding sound radiation, are coupled with turbulent jet noise, producing a very complex sound spectrum. Furthermore, an important effect of the fairing is the non-homogeneous pressure distribution due to the cavity modes excitation, as well as a significant noise reduction [2,3].

Table 1. Ariane 5 acoustic test specification [4]. $P_0 = 2 \cdot 10^{-5}$ Pa.

Octave Band Centre Freq. (Hz)	Ariane 5 Qualifiaction SPL (dB re P_0)	Ariane 5 Acceptance SPL (dB re P_0)	Test Tolerance (dB re P_0)
31.5	132	128	-2, +4
63	134	130	-1, +3
125	139	135	-1, +3
250	143	139	-1, +3
500	138	134	-1, +3
1000	132	128	-1, +3
2000	128	124	-1, +3
Overall SPL	146	142	-1, +3
Test duration	120 s	60 s	0

3 Acoustic testing in space programmes

For simulation and testing purposes, the acoustic load inside the fairing is assumed as a random, stationary and ergodic process. Therefore, the sound signals are described by means of power spectral densities. Spatial characteristics are assimilated to a diffuse field, i.e., the time average of the mean-square pressure is homogeneous and the flow of acoustic energy is equally probable in all directions. For such a field, the pressure cross-spectral density between free-space points or on infinite planes, is given by [5]:

$$S_{x_1 x_2}(k, x) = \sin(kx)/(kx), \tag{1}$$

where k is the wave number and x is the distance between both points.

Sound Pressure Level specification is given in Table 1 for the Ariane 5. These levels are modified depending on the fill factor, the ratio of the maximum spacecraft over fairing cross section areas. For fill factors greater than 60%, a SPL correction of up to +4 dB at 31.5 Hz and +2 dB at 63 Hz shall be applied.

3.1 Test Facilities

Sound pressure loading is customarily tested in reverberating chambers, capable of reproducing the intense sound pressure levels of the launch including safety factors and tolerances. Commercially available reverberating chambers in Europe are listed in Table 2. Other chambers exist, although designed for other applications, such as the chamber of the "Instituto de Acústica – CSIC" at Madrid. It is a 200 m^3 chamber, well suited for development tests, with a 20s reverberation time at 100 Hz, producing 130 dB OASPL with loudspeakers.

The generation of noise in reverberating chambers consists of signal generation and noise power production. The former deals with the source signal driving amplifiers. For random signals, as is the case of launch environment specifications, the signal is usually produced by a white-noise generator and goes through spectrum shaping, band-pass filtering and limiting of peaks. Therefore, the sound measured in the reverberating chamber could be described as white noise within each band, amplified to meet the required SPL as in Table 1.

Table 2. Description of European acoustic test facilities.

Chamber	Dimensions (m) & Volume (m^3)	OASPL (dB re Po)	Reverberation time	Sound production
LEAF	9×11×16.4 1630	155	35 s at 100 Hz	4 modulators & exp. horns. Fluid: N_2
IABG	8.4×10.4×15.2 1380	156	25 s at 100 Hz	3 modulators & exp. horns. Fluid: air
Intespace	8.2×10.3×13 1100	156	30 s	3 modulators & exp. horns. Fluid: N_2

However, the actual spectrum depends on the whole system, including the dynamic response of the chamber in its cavity modes. Obviously, there are infinite spectra within test tolerances, e.g., the raw PSD in Fig. 1, showing the modal behavior of the LEAF chamber. It should be mentioned, that the frequency resolution of the signal is not sufficient to resolve chamber modes. Hence, some of the peaks are cut, while each one may contain several modes.

Moreover, the diffuse character of the field can only be guaranteed above the chamber cut-off frequency, which can be assessed with Schroeder's formula [6]:

$$f_{\lim} = \sqrt{\frac{c^3 T_R}{4 \ln 10 \quad V}}, \tag{2}$$

where V is the volume and T_R the reverberation time, usually approximated with Sabine's formula. This estimate of chamber cut-off is, however, very conservative. More practical values can be obtained by using homogeneity criteria based on control microphones data. Below cut-off, the field in the reverberating chamber is no longer diffuse and could be described by low order cavity modes with their corresponding non-uniform pressure distribution. An immediate question arises concerning the fidelity of sound spectra fulfilling specifications when compared to real flight noise loads, i.e., the noise generated does not match the flight noise spectrum below the fairing. This can be relevant if structural eigenmodes can couple with chamber or fairing cavity modes, especially in the low frequency range.

3.2 Modelling and control of the acoustic input

The diffuse field is usually modelled as a combination of plane waves, with propagation directions distributed in the 4π steradian space [7,8,9]. All waves carry the specified pressure signal and are uncorrelated. Weighting factors may be needed for each incidence direction in order to compensate the different solid angles. The number of waves discretising the diffuse field can range between 14 ($\Delta=\pi/3$) and 62 ($\Delta=\pi/6$) in most common industrial applications, although it is not rare to find 300 or more [9]. The Sommerfeld radiation condition has to be verified with this approach since the chamber walls are not modelled. Alternatively, the modal approach simulates the reverberating field as a superposition of modes. This method is closer to the test reality, although a high price has to be paid for model complexity and tuning to each test facility [10].

The acoustic input is controlled during test performance either manually or by automatic means. The test tolerances are applied to the mean of control microphones (2 to 8 typically) as specified for octave or 1/3 bands in best cases. This may result in pressure PSD differing significantly from the specified inputs when plotted in fine resolution, as in Fig. 1, or showing non-homogeneous distributions within the chamber. This situation is an evident source of errors.

4 Structural response simulation and analysis

Numerical simulation of the vibroacoustic case has been faced at different levels of complexity in the space industry [1]. The simplest approach is the pure structural dynamic simulation without consideration of fluid coupling. The pressure input is then specified as that of a rigid baffled plate for the whole structure, disregarding the diffuse field modelling based on uncorrelated plane waves. This is the most common method in industrial practices, producing very poor correlation results, irrespective of the structural model quality. Some alleviation to this picture is provided by Joint Acceptance Analysis (JAA), allowing for a rapid assessment of the response to diffuse fields. One of the principal applications of JAA is stresses and fatigue analysis [11].

Fidelity can be greatly improved by introducing rigid scattering in the modelling of unbaffled surfaces. This is still an incomplete physical description since it does not model radiation, although very conservative in most cases. For lightweight structures, such as antenna reflectors, radiation coupling must also be taken into account, in addition to rigid scattering and modelling the diffuse field.

A classical linear formulation in the frequency domain, retaining scattering and radiation, can be expressed with Helmholtz equation (3) for the fluid domain, the structure dynamics and constitutive law, interface conditions and Sommerfeld's radiation condition (4):

$$\left(\nabla^2 + k^2\right)P = 0\,, \tag{3}$$

$$\lim_{r\to\infty} r\left(\frac{\partial P}{\partial r} + \mathrm{j}kP\right) = 0\,. \tag{4}$$

Alternatively, an integral form of Helmholtz' equation, based on the free-space Green's function, g, is [12]:

$$P(r) = P_I - 2\iint_{S_0}\left(P(r_0)\frac{\partial g}{\partial n_0} - \rho_f\omega^2\mathbf{w}\cdot\mathbf{n}_0\; g\right)\mathrm{d}S_0\,. \tag{5}$$

Both forms lead to numerical solutions of the coupled problem [13]. Starting with the differential eqn (3), the fluid can be modelled with Finite Elements, as well as the structure, taking account of the fluid/structure coupling. This FEM/FEM procedure is well suited for interior problems, where the fluid is confined and there is no fluid/fluid interface. Exterior problems, however, require treatment of Sommerfeld's radiation condition. Alternatively, the integral eqn (5) results in numerical methods based on variational procedures or

collocation [13], leading to the Boundary Element Method. Coupled BEM/FEM is usually less CPU demanding than FEM/FEM for exterior problems.

Commercial codes exploiting the BEM/FEM technique in the low frequency range end up solving large systems of linear equations containing the structural unknowns. After projection on the structural modes basis, the number of degrees of freedom is considerably reduced. However, the system of equations must be solved for every frequency required, resulting in lengthy computations, unless interpolation is allowed with an impact on accuracy.

5 Signal Processing

A conventional data reduction method for acoustic pressure signals is the Sound Pressure Level in octave-fraction bands:

$$\mathrm{PSD}_K = \frac{1}{\Delta f_K} \int_{f_{K-1}}^{f_K} \mathrm{PSD}(f)\,df, \tag{6}$$

i.e., the mean of PSD in band *K*. The limiting frequencies are upper bounds of the bands. So, the curve is reduced to discrete data in the central frequencies.

A different approach is proposed for pressure signal treatment, that retains more information and better resolution. Since fine resolution PSD reflect the modal behavior of the chamber, they contain a high density of peaks fluctuating around a mean value. This is too much information hiding the signal of interest. Therefore, a zero-phase digital filter has been applied in the frequency domain, with the advantage of maintaining the fine resolution of the original signal and smoothing the chamber modes without totally erasing the information containing structural response. The filter proposed is a forward-backward moving average of the spectral density, hence introducing no frequency shift and preserving resolution [14,15]. The formulation is applied directly in the frequency domain:

$$X_i = \mathrm{PSD}(f_i), \tag{7}$$

$$Y_i = \frac{1}{m^2} \sum_{q=0}^{m-1} \left(\sum_{p=0}^{m-1} X_{i+p-q} \right), \tag{8}$$

where $i = 1,2\ldots n$, m the number of averaged lines and n is the total number of lines in the one-sided PSD signal. This simple filter is applied offline and results from simplifying a more sophisticated FIR filter, designed with these criteria: Direct application in the frequency domain, no frequency shift, no frequency resolution loss and preservation of the energy contents in any frequency band. The simplified filter in eqn (8), fulfils all the requirements, but for a small energy leak estimated as less than 1%. Fig. 1 shows the original pressure PSD signal, corresponding to test control data in the LEAF chamber, together with the filtered and octave band averaged curves. Pressure oscillations are higher at low frequencies, where diffusion is not guaranteed, despite fulfilling tolerances. Obviously, the filtered signal provides a better idea of the actual pressure signal than the octave or even 1/3 octave average.

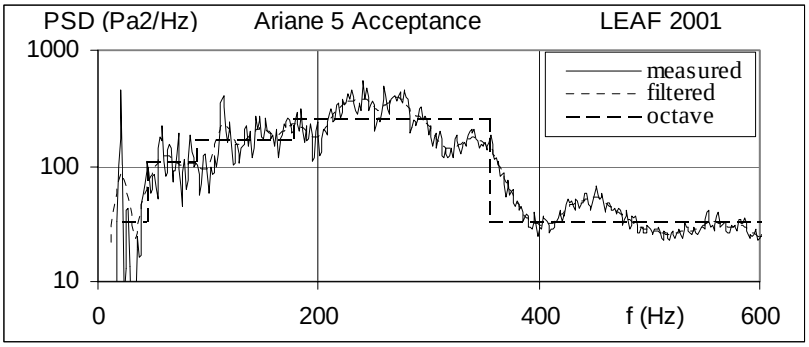

Fig. 1. Direct pressure measurement, filtered and octave band averaged data.

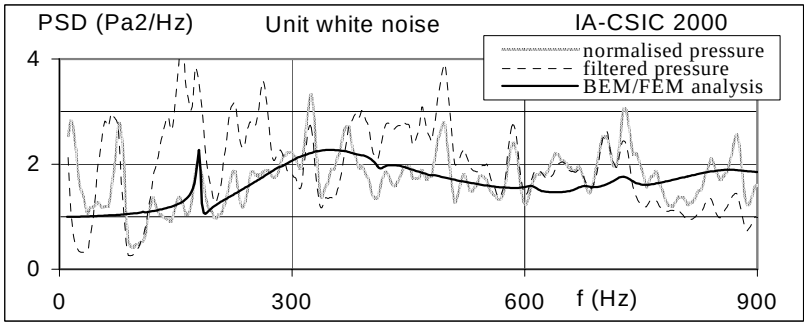

Fig. 2. Circular plate. Measured pressure at centre before and after normalisation.

Whenever correlation with analysis or comparison between different tests is required, a normalisation operation must be considered. This is so because of the difficulty in the realisation of tests, in particular for the repeatability of input loads. Fig. 2 shows the effect of normalisation in a typical test, described later on, for a unit white noise input. In order to define the normalisation factor, care must be exercised in selecting the control signals and the filtering or averaging method. In common industrial practice, octave band averaging of pressure is the selected method. However, fine resolution should be used for better correlation.

6 Correlation examples

Two specimens are used for analysis/test correlation [15]: a circular plate (diameter a = 0.7 m) and a large antenna reflector. The circular plate is a Carbon fibre reinforced sandwich with 6 mm thick honeycomb core. The IOLA reflector, belonging to the ARTEMIS spacecraft, is a 2.8 m parabolic surface with a shell similar to plate B and a stiffening back structure (Fig. 3).
Tests have been performed in the chamber of the 'Instituto de Acustica' and the LEAF at ESA-ESTEC. The numerical analysis has been carried out with a validated commercial BEM code running on a UNIX workstation.

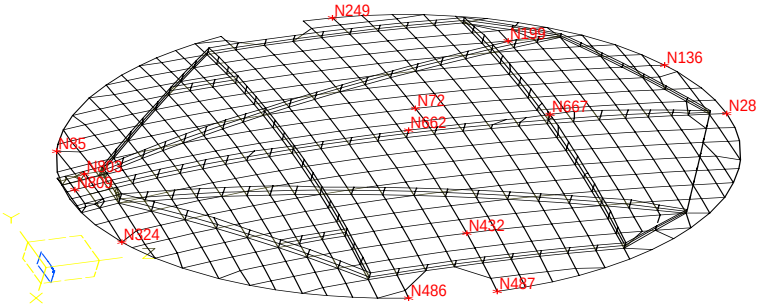

Fig. 3. IOLA reflector fluid model (EADS CASA Espacio).

Fig. 2 shows measured and calculated pressure PSD at the centre of the plate. The input is a 1 Pa^2/Hz white noise up to 1000 Hz. The non-diffusion of the chamber is causing divergence from the calculated pressure, in spite of careful normalisation of test data and control signal screening. Especially, the excitation of chamber modes between 20 and 80 Hz is hardly controllable. Despite the apparent mismatch in pressure, accelerations correlate fairly well with analytical prediction, as shown in Figs. 4 and 5. In particular, mode (0,1) lies within the blocked pressure excitation band with a high joint acceptance and, hence, dominates the response [8,15]. This fact is well captured by analysis. The quantitative response at resonances, except for damping factors to be further tuned, is driven by the character of the input pressure. The precise value is highly affected by the matching with chamber pressure peaks, making the correlation task almost useless in such terms. Nevertheless, the result far better than the one obtained with octave band reduction of the input reference.

Concerning the IOLA reflector, despite the higher modal density, good correlation is obtained by applying the mentioned procedures, for both PSD curves (Fig. 6) and RMS values (Table 3). The test shown is an Ariane 5 Acceptance profile in free-free boundary conditions.

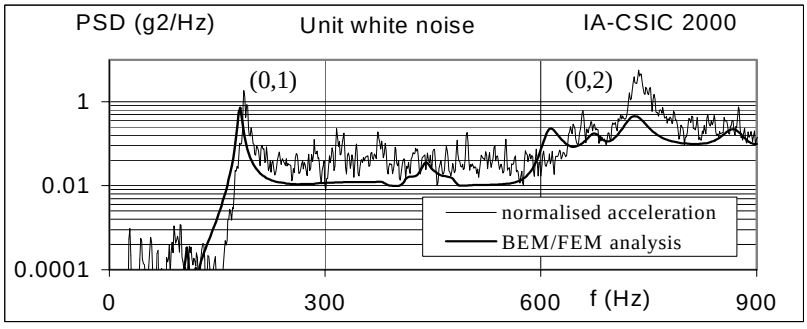

Fig. 4. Circular plate in free-free conditions. Acceleration PSD at the centre.

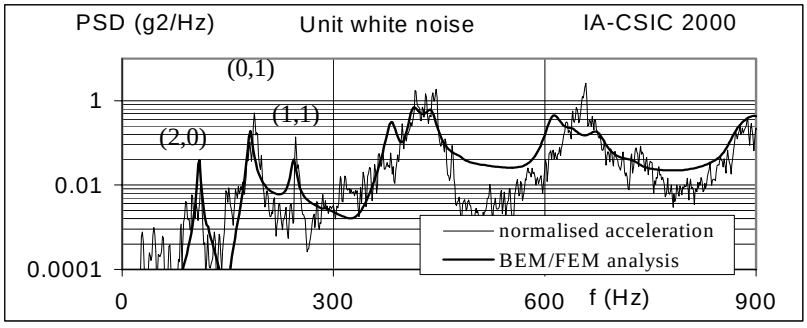

Fig. 5. Circular plate in free-free conditions. Acceleration at edge.

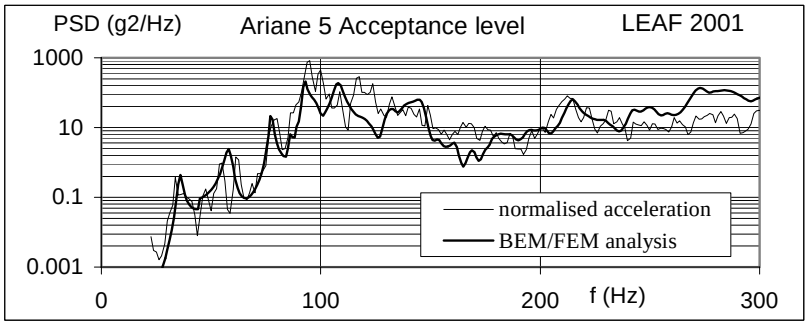

Fig. 6. IOLA in free-free conditions. Acceleration at edge (N249).

Table 3. IOLA reflector. RMS acceleration (g). Range: 1-355 Hz.

Accelerometer	Test: Ariane 5 Accept.	Analysis
N249	98.9	96.8
N85	99.5	102.6
N72	73.4	92.8
N486	83.2	96.3

7 Conclusions

Correlation of analytical predictions and measurements of vibroacoustic response of spacecraft is a task submitted to many sources of uncertainty, mostly related to specifications, test procedures and limitations of test facilities and analysis tools. In order to better explain the discrepancies, a careful review of common industrial practices has been performed, pointing out the sources of error and proposing new signal processing methods. These consist of improving resolution and taking account of the differences between reverberating and diffuse fields. In particular, control signal definition based on homogeneity and normalisation to a sensible reference, together with digital filtering techniques allow for a better understanding of the low-frequency behaviour of structures in reverberating chambers.

8 Acknowledgements

The authors thank A. Moreno, C. de la Colina, R. Rodriguez, F. Simon, J. Pfretzschner (Instituto de Acustica) and R. Garcia (ESA) for their contributions.

9 References

[1] Stavrinidis, C., Witting, M. & Klein, M. Advancements in Vibroacoustic Evaluation of Satellite Structures. *Acta Astronautica*, **48(4)**, 203-210, 2001.

[2] Chemoul, B., Louaas, E., Roux, P., Schmitt, D. & Pourcher, M. Ariane 5 Flight Environments. *Acta Astronautica*, **48(5)**, 275-285, 2001.

[3] Faust, M. & Piret, G., Vibro-Acoustic Payload Effect Test of the Ariane 5 Fairing with Olympus Satellite in ESTEC-LEAF. *Proc. of the Conference on Spacecraft Structures, Materials & Mechanical Testing* (ESA-SP 386), 1996.

[4] *Ariane 5 User's Manual*. Issue 3, Rev. 0. Arianespace, Paris, March 2000.

[5] Bodlund, K. A New Quantity for Comparative Measurements Concerning the Diffusion of Stationary Sound Fields, *Journal of Sound and Vibration*, **44(2)**, 191-207, 1976.

[6] Schroeder, M. Statistik der Frequenzkurve in Raeumen. *Acustica*, **4**, 594-600, 1954.

[7] Witting, M. *Modelling of Diffuse Sound Field Excitations & Dynamic Analysis of Lightweight Structures*. Ph.D. Thesis, TU Muenchen, 1999.

[8] Rioboo, J.L., Santiago-Prowald, J. & Garcia, R. Qualitative Vibroacoustic Response Prediction of Antenna-Like Structures During Launch into Orbit. *Proc. of the Eur. Conference on Spacecraft Structures, Materials & Mechanical Testing*, (ESA-SP 468) Noordwijk, The Netherlands, Dec. 2000.

[9] Nelisse, H., Beslin, O. & Nicolas, J. Fluid-Structure Coupling for an Unbaffled Elastic Panel in a Diffuse Field. *Journal of Sound and Vibration*. **198(4)**, 485-506. 1996.

[10] Nelisse, H., Beslin , O. & Nicolas, J. Panel Dynamic Response to a Reverberant Acoustic Field, *AIAA Journal*. V. 33, N. 9, 1590-1596, 1995.

[11] Wallace, C.E. Structural Response and Acoustic Fatigue for Random Progressive Waves & Diffuse Fields, *Journal of Spacecraft and Rockets*, V. 22, N. 3, 340-344, 1985.

[12] Junger, M.C. & Feit, D. *Sound, Structures and Their Interaction*. MIT Press. Cambridge, Mass. and London, England, 1972.

[13] Hamdi, M.A. Méthodes de Discrétisation par Éléments Finis et Éléments de Frontière (Ch. 9). *Rayonnement Acoustique de Structures: Vibroacoustique, Interaction Fluide-Structure*, ed. Lesueur, C. Editiones Eyrolles, Paris, 1988.

[14] De la Colina, C. *Respuesta acústica vibratoria de estructuras aerospaciales*. Technical note for CASA Espacio. Instituto de Acustica-CSIC, March 2000.

[15] Rioboo, J., Santiago-Prowald, J. *LARDAL Summary Report*. ESA document CAS-LAR-TNO17, 2002.